

Quantum Mpemba effect in a four-site Bose-Hubbard model

Asad Ali^{1, *}, M.I. Hussain¹, Hamid Arian Zad², H. Kuniyil¹,

M. T. Rahim¹, Saif Al-Kuwari^{1, †} and Saeed Haddadi^{3, ‡}

¹*Qatar Center for Quantum Computing, College of Science and Engineering, Hamad Bin Khalifa University, Doha, Qatar*

²*Department of Theoretical Physics and Astrophysics,*

Faculty of Science of P. J. Šafárik University, Park Angelinum 9, 040 01 Košice, Slovak Republic

³*School of Particles and Accelerators, Institute for Research in*

Fundamental Sciences (IPM), P.O. Box 19395-5531, Tehran, Iran

(Dated: September 9, 2025)

We investigated the quantum Mpemba effect (QME) in a one-dimensional Bose-Hubbard model across clean and disordered regimes using exact numerical technique of a four-site lattice under Lindblad dynamics with local dephasing noise. By systematically varying hopping strength, onsite interactions, Stark potentials, and random disorder, we probe relaxation dynamics toward a common steady state using trace distance, relative entropy, entanglement asymmetry, and ℓ_1 -norm of coherence metrics. Our results reveal that QME emerges prominently in the clean-interacting regime, where many-body correlations drive nonlinear relaxation pathways, enabling initially distant states to overtake closer ones. In contrast, non-interacting systems exhibit conventional thermalization, whereas Stark potentials and random disorder suppress QME by inducing localization barriers, with disorder causing milder delays compared to the pronounced effects of Stark fields. Entanglement asymmetry proves to be particularly sensitive to the symmetry restoration dynamics underlying QME. These findings elucidate the critical role of interactions in anomalous relaxation and provide insights for controlling quantum thermalization in experimental platforms such as ultra-cold atomic systems.

Keywords: quantum Mpemba effect, Bose-Hubbard model, Stark potential, Quantum thermalization

I. INTRODUCTION

Thermodynamic equilibrium during gradual temperature changes dictates that cooling occurs incrementally through all intermediate temperatures, with colder objects reaching equilibrium faster than hotter ones. The Mpemba effect [1] contradicts this fundamental expectation: hot samples can cool faster than colder ones under certain conditions. This counterintuitive phenomenon, documented since Aristotle [2] and later by Descartes [3] and Bacon [4], remains controversial [5, 6] despite extensive investigation.

The universality of the Mpemba effect has been demonstrated in various classical systems, including clathrate hydrates [7], polymer systems [8], magnetic alloys [9], carbon nanotube mechanical resonators [10], granular gases [11], and dilute atomic gases [12]. A significant theoretical breakthrough emerged from stochastic thermodynamics, revealing that relaxation dynamics are fundamentally determined by the system's slowest decaying eigenmode [13, 14]. The Mpemba effect manifests when the initial states at higher temperatures exhibit reduced overlap with this critical mode. The most dramatic manifestation, termed the strong Mpemba effect, occurs when this overlap vanishes entirely, resulting in exponential acceleration of the relaxation process [14].

The quantum realm offers a particularly fertile ground for investigating analogous phenomena. The scenario wherein a quantum system initially farther from equilibrium relaxes faster than a system initialized closer to equilibrium, so-called the quantum Mpemba effect (QME). This broad definition encompasses both cooling and heating processes (the latter termed the inverse Mpemba effect) and spans two distinct classes of quantum systems. The first class involves open quantum systems where relaxation is governed by classical-like fluctuations through environmental coupling and Lindbladian master equation dynamics. The second encompasses closed quantum systems undergoing unitary evolution following quantum quenches, where relaxation is driven entirely by quantum fluctuations. This duality creates a unifying framework that connects classical-like relaxation dynamics with uniquely quantum processes.

The theoretical understanding of QME involves several distinct but potentially complementary mechanisms. The strong Mpemba effect occurs when the initial quantum state exhibits negligible overlap with the slowest-decaying mode of the Liouvillian superoperator, enabling exponential acceleration of relaxation dynamics [15, 16]. Non-normal Liouvillian dynamics can induce transient interference effects between distinct decaying modes, leading to anomalous relaxation behavior [17]. Initial system-environment correlations or non-Markovian memory effects can significantly accelerate equilibration [18]. In closed systems, symmetry restoration through entanglement asymmetry evolution can drive QME manifestation [18, 19]. Additionally, quantum integrability and associated quantum fluctuation

* asal68826@hbku.edu.qa

† smalkuwari@hbku.edu.qa

‡ haddadi@ipm.ir

effects contribute to QME through distinct relaxation pathways compared to chaotic systems [18, 20].

Recent experimental advances have provided compelling demonstrations of QME. Joshi et al. observed QME in a 12-ion quantum simulator for the first time, employing entanglement asymmetry as the primary observable for monitoring symmetry restoration dynamics [21]. On the other hand, Zhang et al. achieved the first definitive observation of strong QME using a single trapped-ion system with a carefully engineered three-level structure [15]. An inverse QME has also been demonstrated experimentally, where an initially colder quantum state achieved thermal equilibrium faster than a comparatively warmer initial state [22].

Motivated by this rich phenomenology, we investigate QME in the paradigmatic one-dimensional Bose-Hubbard model (BHM) in the presence and absence of spatial disorder and external driving fields. We explore whether QME emerges in a disordered system subjected to a linear Stark potential, focusing on dephasing noise. Our investigation provides a systematic identification with particular emphasis on the interplay between localization phenomena and anomalous relaxation dynamics. Additionally, we investigate the quantification traces of QME manifestations, employing multiple distance measures from the equilibrium [18]. This includes trace distance, quantum relative entropy, entanglement asymmetry, and quantum coherence-based metrics, which quantify the strength and dependence of QME on the chosen metric.

The organization of this paper is as follows: Sec. II presents the theoretical model and describes the metrics used to characterize QME. The detailed procedure to solve the model and enrich the outcomes is described in Sec. III. In Sec. IV we discuss the most important results gained from our investigations, and Sec. V provides conclusions and future outlook.

II. MODEL AND METHODS

We investigate the relaxation dynamics of interacting bosons on a one-dimensional lattice described by the Bose-Hubbard Hamiltonian:

$$\begin{aligned} \hat{H}_{\text{BH}} = & -\tau \sum_{j=1}^{N-1} \left(\hat{a}_j^\dagger \hat{a}_{j+1} + \hat{a}_{j+1}^\dagger \hat{a}_j \right) \\ & -\mu \sum_{j=1}^N \hat{n}_j + \frac{U}{2} \sum_{j=1}^N \hat{n}_j (\hat{n}_j - 1), \end{aligned} \quad (1)$$

where N is the number of sites and particles, \hat{a}_j^\dagger (\hat{a}_j) creates (annihilates) a boson at site j , $\hat{n}_j = \hat{a}_j^\dagger \hat{a}_j$ is the number operator. Parameters τ , μ , and U denote the tunneling amplitude, chemical potential, and on-site interaction strength, respectively. The competition between tunneling and interactions drives a quantum phase transition between superfluid and Mott insulator phases. To

incorporate environmental effects and external fields, we extend the Hamiltonian as

$$\hat{H} = \hat{H}_{\text{BH}} + \sum_{j=1}^N (gj + \delta_j) \hat{n}_j, \quad (2)$$

where g is the strength of the linear Stark field and δ_j represents a site-dependent disorder uniformly distributed in $[-\delta, +\delta]$ [23].

The system's coupling to an external environment causes decoherence that under the Markovian approximation is modeled through the Lindblad master equation:

$$\begin{aligned} \frac{d\hat{\rho}(t)}{dt} = & \mathcal{L}[\hat{\rho}(t)] \\ = & -i[\hat{H}, \hat{\rho}(t)] + \sum_k \left(\hat{L}_k \hat{\rho}(t) \hat{L}_k^\dagger - \frac{1}{2} \{ \hat{L}_k^\dagger \hat{L}_k, \hat{\rho}(t) \} \right), \end{aligned} \quad (3)$$

where \mathcal{L} is the Liouvillian superoperator and \hat{L}_k are Lindblad operators characterizing the system-environment interaction. The steady state $\hat{\rho}_{\text{ss}}$ satisfies $\mathcal{L}[\hat{\rho}_{\text{ss}}] = 0$. We consider dephasing as the primary dissipative mechanism, modeled by $\hat{L}_j = \sqrt{\gamma} \hat{n}_j$, where γ is the dephasing rate acting on the local particle number at each site j , reflecting realistic experimental conditions.

The density matrix evolution admits a spectral decomposition in terms of the Liouvillian eigenmodes:

$$\hat{\rho}(t) = \hat{\rho}_{\text{ss}} + \sum_{j=1}^{N-1} c_j e^{\lambda_j t} \hat{\rho}_j, \quad (4)$$

where λ_j are the non-zero eigenvalues of \mathcal{L} with $\text{Re}(\lambda_j) < 0$, $\hat{\rho}_j$ are the corresponding eigenmatrices, and the coefficients c_j depend on the initial state $\hat{\rho}(0)$. The eigenmode with the largest real part determines the asymptotic approach to the steady state.

The QME represents a non-equilibrium phenomenon where a system initialized farther from equilibrium relaxes faster than one prepared closer to equilibrium. Formally, consider two initial states $\hat{\rho}_1(0)$ and $\hat{\rho}_2(0)$ evolving toward a steady state $\hat{\rho}_{\text{ss}}$ under unitary or dissipative dynamics. The QME occurs when there exists a crossing time $t_M > 0$ such that for all $t > t_M$, the ordering of certain distance metric d from equilibrium inverts: $d(\hat{\rho}_1(0), \hat{\rho}_{\text{ss}}) > d(\hat{\rho}_2(0), \hat{\rho}_{\text{ss}})$ but $d(\hat{\rho}_1(t), \hat{\rho}_{\text{ss}}) < d(\hat{\rho}_2(t), \hat{\rho}_{\text{ss}})$ where $d(\cdot, \cdot)$ denotes a well-defined distance measure on the space of quantum states. The strong Mpemba effect constitutes a special case where $\hat{\rho}_1(0)$ exhibits exponentially faster relaxation due to vanishing overlap with the system's slowest-decaying eigenmode, a condition that can be systematically engineered through appropriate state preparation protocols [15, 16].

The characterization of QME necessitates careful selection of distance metrics that capture different aspects of the relaxation dynamics. The trace distance provides a

natural geometric measure of distinguishability between quantum states:

$$D[\hat{\rho}(t), \hat{\rho}_{\text{ss}}] = \frac{1}{2} \text{Tr} \left[\sqrt{(\hat{\rho}(t) - \hat{\rho}_{\text{ss}})^\dagger (\hat{\rho}(t) - \hat{\rho}_{\text{ss}})} \right]. \quad (5)$$

This metric enjoys several advantageous properties: it is contractive under completely positive trace-preserving maps, bounded between 0 and 1, and has a direct operational interpretation as the optimal distinguishability in quantum hypothesis testing [24].

From a thermodynamic perspective, the quantum relative entropy offers an information-theoretic measure of nonequilibrium:

$$S[\hat{\rho}(t) || \hat{\rho}_{\text{ss}}] = \text{Tr} [\hat{\rho}(t) (\log \hat{\rho}(t) - \log \hat{\rho}_{\text{ss}})]. \quad (6)$$

This quantity connects to non-equilibrium free energy differences and satisfies monotonicity under quantum channels, making it particularly suitable for studying open quantum system dynamics [25].

Entanglement asymmetry serves as a powerful diagnostic of symmetry restoration dynamics. Given a subsystem A and its complement \bar{A} , we define the Rényi entanglement asymmetry of order n as:

$$\Delta S_A^{(n)}(t) = S^{(n)}(\rho_{A,Q}(t)) - S^{(n)}(\rho_A(t)), \quad (7)$$

where $\rho_A(t) = \text{Tr}_{\bar{A}}[\hat{\rho}(t)]$ is the reduced density matrix, and $\rho_{A,Q}(t)$ represents its symmetrized version with respect to a conserved charge operator Q :

$$\rho_{A,Q}(t) = \sum_q \Pi_q \rho_A(t) \Pi_q. \quad (8)$$

Here, Π_q projects onto the eigenspace of $Q_A = \sum_{i \in A} \hat{n}_i$ (where \hat{n}_i is the particle number operator at site i , and the sum runs over all sites in subsystem A) with eigenvalue q , and $S^{(n)}(\rho) = (1 - n)^{-1} \log \text{Tr}(\rho^n)$ denotes the Rényi entropy. We take $n = 1$ that corresponds to von Neumann entropy. The entanglement asymmetry $\Delta S_A^{(n)}(t)$ vanishes precisely when $\rho_A(t)$ is paired with Q_A , providing a sensitive measure of symmetry breaking and restoration [21].

The dynamical behavior of these metrics reveals distinct aspects of QME. Trace distance and relative entropy capture a global approach to equilibrium, while quantum coherence measures track quantum superposition dynamics. Entanglement asymmetry specifically probes how local subsystems regain symmetry during thermalization. The strong Mpemba effect manifests itself most dramatically in entanglement asymmetry dynamics, where initial states with greater symmetry breaking can exhibit faster symmetry restoration [26, 27]. Experimental protocols for measuring these quantities range from quantum state tomography [28] to randomized measurement techniques

[29], with recent advances enabling direct observation of QME in trapped-ion platforms [21].

Quantum coherence represents another crucial dimension of relaxation dynamics. This measure quantifies the preferred basis of the total superposition content:

$$\mathcal{C}[\hat{\rho}(t)] = \sum_{i \neq j} |\langle i | \hat{\rho}(t) | j \rangle|, \quad (9)$$

where $\{|i\rangle\}$ denotes the Fock basis. This measure has proven sensitive to dynamical phase transitions and exhibits characteristic scaling during thermalization processes [30].

The choice of metric significantly influences QME observation, as different measures may exhibit crossing at distinct times or even qualitatively different behavior. This metric dependence underscores the multifaceted nature of quantum thermalization and highlights the importance of selecting appropriate observables for specific experimental implementations [18, 25]. Theoretical analyses typically employ multiple complementary measures to establish robust signatures of QME across different physical scenarios.

Throughout this work, we focus on the unit-filling configuration with $N = L = 4$ bosons on four lattice sites and a chemical potential $\mu = 0.5$, corresponding to the center of the first Mott lobe in the phase diagram of BHM. This choice results in a Hilbert space of dimension $D = 35$, while the associated Liouvillian superoperator has dimension $D^2 = 1225$, reflecting the increased complexity of the open-system dynamics. Given the combinatorial growth of the state space under exact diagonalization and the added cost of solving the full Lindblad master equation, we restrict our analysis to this minimal yet non-trivial setting. Despite its modest size, this setup retains the essential ingredients to capture symmetry-breaking dynamics and dissipative effects in a controlled and numerically exact manner.

III. PROCEDURE FOR PROBING QME

To systematically investigate the emergence and characteristics of the QME in the four-site BHM, we employ a controlled numerical procedure. This procedure is designed to isolate the individual and combined roles of kinetic energy (τ), many-body interactions (U), and spatial inhomogeneity (g, δ) in driving anomalous relaxation dynamics under dissipative Lindblad evolution. The core of the investigation involves preparing a hierarchy of initial states with varying distances from a predefined common steady state and tracking their relaxation using multiple complementary quantum metrics to identify crossover events indicative of the QME.

The procedure is implemented through the following sequential steps:

A. System Specification and Parameter Regimes

We define a four-site lattice with unit filling of four particles ($N = 4$), enforced by setting the chemical potential to be fixed as $\mu = 0.5$. The system's Hamiltonian is given by Eq. (2). We explore four distinct physical regimes by selectively activating parameters:

- **Clean, Non-interacting:** $U = 0$, $g = 0$, $\delta = 0$. The hopping strength τ is the control variable.
- **Clean, Interacting:** $U > 0$ (fixed), $g = 0$, $\delta = 0$. The hopping strength τ is the control variable.
- **Stark Potential:** $U > 0$ (fixed), τ (fixed, low), $\delta = 0$. The Stark field strength g is the control variable.
- **Random Disorder:** $U > 0$ (fixed), τ (fixed, low), $g = 0$. The disorder amplitude δ is the control variable.

For a chosen regime, a set of thermal initial states $\{\hat{\rho}_\beta^\theta\}$ is prepared. Each state is a Gibbs state $\hat{\rho}_\beta^\theta = e^{-\beta \hat{H}^\theta} / \mathcal{Z}^\theta$ with $\mathcal{Z}^\theta = \text{Tr}(e^{-\beta \hat{H}^\theta})$ at a fixed inverse temperature β , where the Hamiltonian parameter θ (which is τ , g , or δ) is varied to create a spectrum of initial conditions. This generates a family of states with systematically varying initial properties (e.g., delocalization, interaction energy, or potential energy) while maintaining a fixed temperature.

B. Quantification of Relaxation Dynamics

A single reference steady state $\hat{\rho}_{ss} \equiv \hat{\rho}_{ss}^{\theta_{\text{ref}}}$ is defined for each regime. This is the state that satisfies $\mathcal{L}[\hat{\rho}_{ss}] = 0$ for a fixed reference value of the control parameter θ_{ref} (e.g., a specific τ_{ref} , g_{ref} , or δ_{ref}), under the same Lindblad dynamics used for time evolution. All initial states $\hat{\rho}_\beta^\theta$ are evolved towards this common $\hat{\rho}_{ss}$.

Each initial state $\hat{\rho}(0) = \hat{\rho}_\beta^\theta$ is time-evolved according to the Lindblad master equation (Eq. (3)) with local dephasing operators $\hat{L}_j = \sqrt{\gamma} \hat{n}_j$ and a fixed dephasing rate γ . The equation is solved numerically to obtain the exact time-dependent density matrix $\hat{\rho}(t)$ for each initial condition [31–33].

The distance from the steady state is tracked as a function of time using four distinct metrics, providing a multifaceted view of the relaxation process:

- **Trace Distance:** $D[\hat{\rho}(t), \hat{\rho}_{ss}]$ quantifies the geometric distinguishability.
- **Relative Entropy:** $S[\hat{\rho}(t) || \hat{\rho}_{ss}]$ measures the information-theoretic divergence.
- **Entanglement Asymmetry:** $\Delta S_A^{(n)}(t)$ probes the dynamics of symmetry restoration with respect to the total particle number in a subsystem.

- **ℓ_1 -norm of Coherence:** $\mathcal{C}[\hat{\rho}(t)]$ tracks the decay of quantum superpositions.

C. Identification of the QME

The QME is identified by a characteristic crossing in the time evolution of the distance metrics. Specifically, for two initial states $\hat{\rho}_\beta^{\theta_1}$ and $\hat{\rho}_\beta^{\theta_2}$, the effect is confirmed if:

$$d(\hat{\rho}_\beta^{\theta_1}, \hat{\rho}_{ss}) > d(\hat{\rho}_\beta^{\theta_2}, \hat{\rho}_{ss}) \quad \text{at } t = 0,$$

but there exists a finite time $t_M > 0$ such that for $t > t_M$,

$$d(\hat{\rho}_\beta^{\theta_1}(t), \hat{\rho}_{ss}) < d(\hat{\rho}_\beta^{\theta_2}(t), \hat{\rho}_{ss}),$$

where $d(\cdot, \cdot)$ represents any of the chosen metrics. The consistency of this crossover across multiple metrics is used to verify the robust presence of the QME.

This structured procedure allows for a controlled and comparative analysis of how different physical parameters influence the approach to equilibrium, enabling us to pinpoint the essential ingredients for the counterintuitive relaxation dynamics that define the QME.

IV. RESULTS AND DISCUSSION

A. Clean Tight-Binding Regime

Following the general procedure outlined in Sec. III, we initiate our investigation of the QME by examining the clean non-interacting BHM, setting onsite interaction, disorder, and Stark potential to zero ($U = \delta = g = 0$) with a chemical potential ensuring unit filling. This configuration isolates purely kinetic effects, serving as a baseline to elucidate the role of interactions in quantum thermalization dynamics.

We implement the procedure using a four-site bosonic chain with four particles. Initial thermal states are prepared at a fixed temperature, each characterized by a distinct hopping strength, and evolved under Lindblad dynamics with local dephasing noise acting on particle number operators. All systems converge toward a common reference steady state defined by a specific hopping strength. This approach establishes a hierarchy of initial states with varying degrees of delocalization while preserving identical thermal properties, isolating quantum effects from classical thermal phenomena. Relaxation dynamics are tracked using four complementary quantum metrics: trace distance $D[\hat{\rho}_{ss}, \hat{\rho}(t)]$ to quantify geometric distinguishability, relative entropy $S[\hat{\rho}(t) || \hat{\rho}_{ss}]$ for information-theoretic divergence, entanglement asymmetry ΔS_A for a chosen bipartition to probe particle number symmetry restoration, and ℓ_1 -norm quantum coherence, $\mathcal{C}[\hat{\rho}(t)]$, in the Fock basis to capture quantum superposition dynamics.

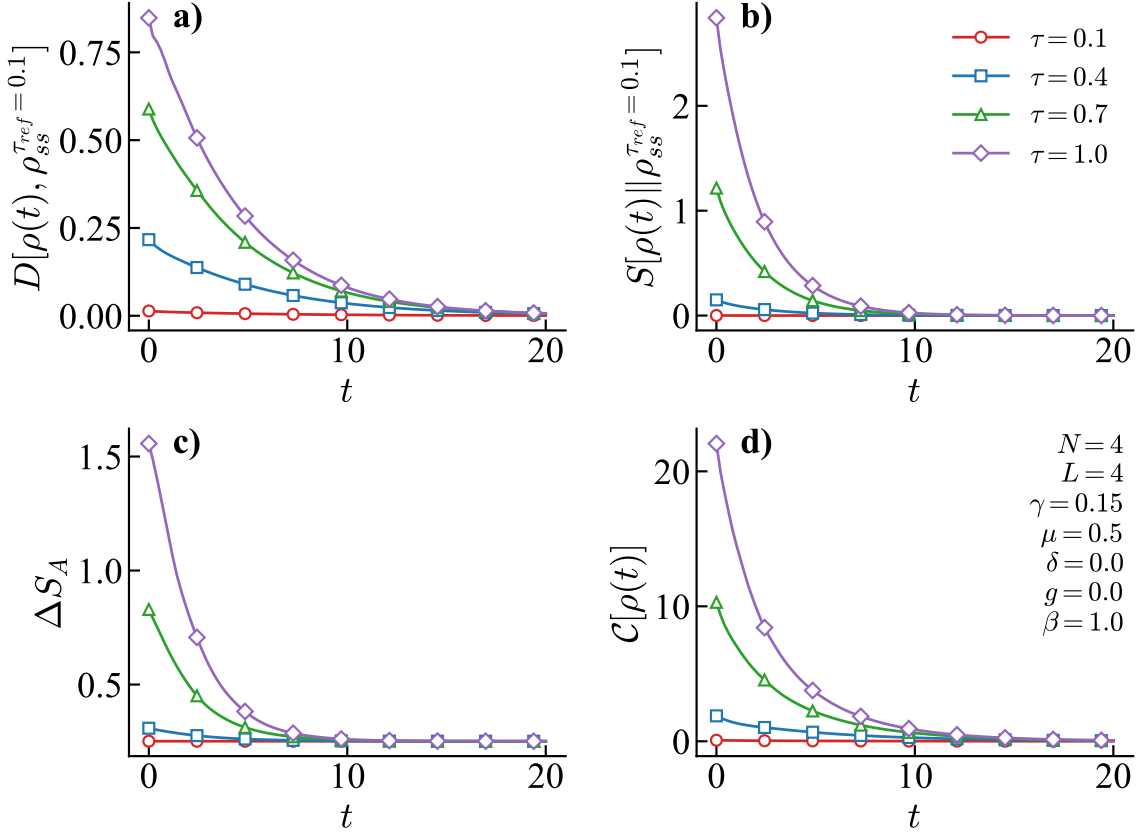


FIG. 1. Absence of the QME in the non-interacting regime ($U = 0$). Relaxation dynamics of a dissipative bosonic system under varying hopping strengths τ . A four-site BHM evolves from thermal initial states under Lindblad dynamics with local dephasing noise (rate γ). The reference steady state $\hat{\rho}_{ss}$ corresponds to a fixed hopping strength τ_{ref} . All four metrics show consistent monotonic relaxation without crossovers: (a) trace distance $D[\hat{\rho}_{ss}, \hat{\rho}(t)]$ measuring distinguishability, (b) relative entropy $S[\hat{\rho}(t)||\hat{\rho}_{ss}]$ quantifying information-theoretic divergence, (c) entanglement asymmetry ΔS_A for bipartition A characterizing particle number symmetry breaking, and (d) ℓ_1 -norm quantum coherence $C[\hat{\rho}(t)]$ in the Fock basis. States initially closer to the steady state (lower τ) maintain their proximity advantage throughout evolution, demonstrating conventional thermalization and highlighting the necessity of interactions for QME emergence. Other parameters $\mu = 0.50$, $U = 0$, $\delta = 0$, $g = 0$, and fixed inverse temperature $\beta = 1$ have been assumed.

The results, shown in Fig. 1, reveal the absence of QME signatures in the non-interacting regime. All quantum metrics exhibit monotonic ordering throughout the evolution, with initial states closer to the reference steady state consistently maintaining their proximity advantage. Specifically, the trace distance in panel 1(a) displays a clear hierarchy, with no crossover events indicative of anomalous relaxation. This ordering persists across relative entropy [panel 1(b)], entanglement asymmetry [panel 1(c)], and quantum coherence [panel 1(d)], confirming conventional thermalization where initial proximity to equilibrium dictates relaxation speed.

Notably, entanglement asymmetry indicates that systems with higher hopping strengths exhibit greater initial symmetry breaking, which persists throughout relaxation, suggesting that symmetry-breaking content hinders convergence to the symmetric steady state. The absence of crossover behavior establishes that kinetic effects alone are insufficient to induce QME, underscoring

the necessity of interactions for anomalous relaxation dynamics in this model.

B. Clean Bose-Hubbard Regime

Building on the non-interacting case explored in Sec. IV A, we extend our investigation of the QME by introducing onsite interactions to the clean Bose-Hubbard model, following the procedure outlined in Sec. III. We maintain zero disorder and Stark potential ($\delta = g = 0$) and a chemical potential ensuring unit filling, isolating the role of many-body correlations in quantum thermalization dynamics and contrasting with the purely kinetic effects of the non-interacting regime.

The onsite interaction term imposes an energy penalty for multiple occupancy per site, reshaping the energy landscape and introducing a competition between kinetic delocalization, driven by hopping, and interaction-

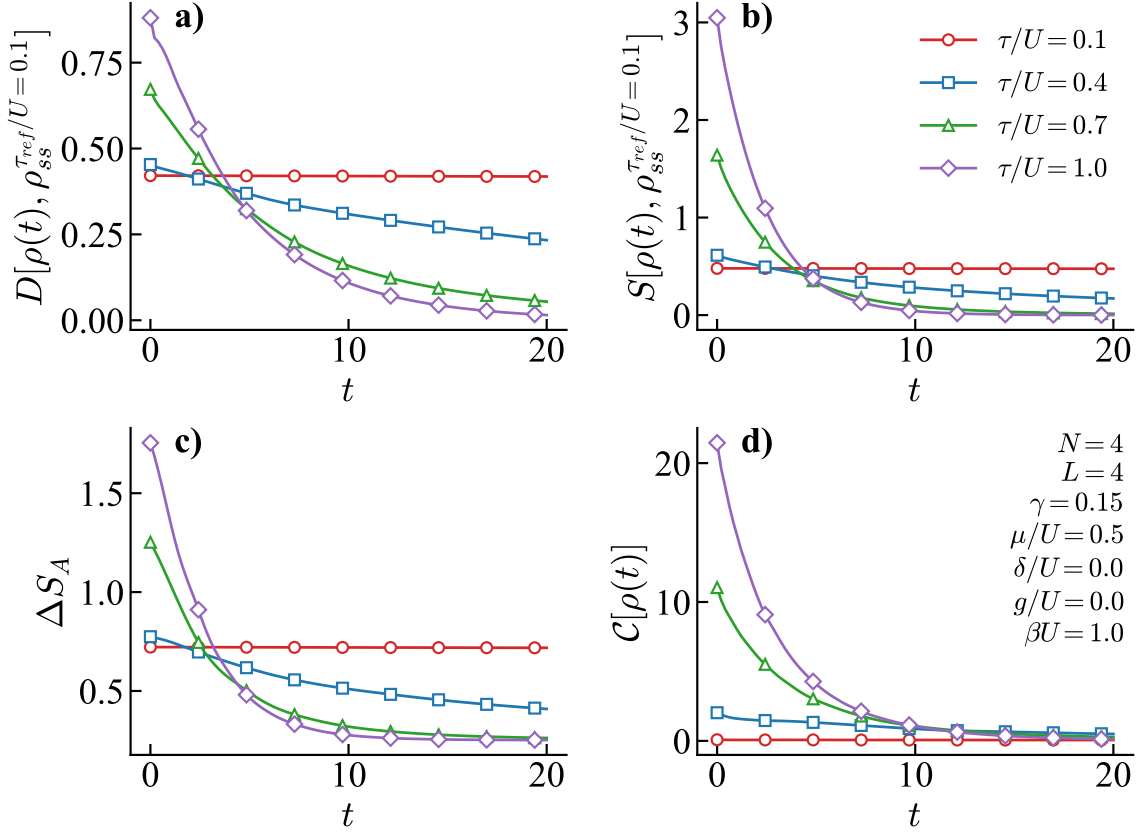


FIG. 2. Emergence of the quantum Mpemba effect in the interacting regime. Relaxation dynamics of a dissipative bosonic chain under varying hopping strengths τ with finite onsite interactions. A four-site system ($L = 4$, $N = 4$) evolves from thermal initial states under Lindblad dynamics with local dephasing noise (rate γ). The reference steady state $\hat{\rho}_{ss}$ corresponds to a fixed hopping strength τ_{ref} . All four metrics exhibit characteristic crossover behavior indicative of QME: **(a)** trace distance $D[\hat{\rho}_{ss}, \hat{\rho}(t)]$ showing inversion of relaxation hierarchy, **(b)** relative entropy $S[\hat{\rho}(t)||\hat{\rho}_{ss}]$ demonstrating faster convergence for initially more distant states, **(c)** entanglement asymmetry ΔS_A for bipartition A revealing enhanced symmetry restoration dynamics, and **(d)** ℓ_1 -norm quantum coherence $\mathcal{C}[\hat{\rho}(t)]$ in the Fock basis showing interaction-modified decoherence pathways. States initially farther from equilibrium (higher τ) overtake closer ones, demonstrating anomalous thermalization enabled by many-body interactions. Parameters: $\mu = 0.50$, $U > 0$ (fixed), $\delta = 0$, $g = 0$, fixed inverse temperature $\beta U = 1$.

induced localization, driven by onsite repulsion. At unit filling, this competition is well-documented to heighten sensitivity to correlation effects, making this regime ideal for probing interaction-driven QME.

We implement the procedure using a four-site bosonic chain with an equal number of particles. Initial thermal states are prepared at a fixed inverse temperature, each characterized by a distinct hopping strength, and evolved under Lindblad dynamics with local dephasing noise acting on particle number operators, consistent with the setup in Sec. IV A. All systems converge toward a common reference steady state defined by a specific hopping strength. Relaxation dynamics are monitored using four quantum metrics: trace distance $D[\hat{\rho}_{ss}, \hat{\rho}(t)]$ for geometric distinguishability, relative entropy $S[\hat{\rho}(t)||\hat{\rho}_{ss}]$ for information-theoretic divergence, entanglement asymmetry ΔS_A for a chosen bipartition to assess particle number symmetry restoration, and ℓ_1 -norm quantum coherence $\mathcal{C}[\hat{\rho}(t)]$ in the Fock basis to capture quantum super-

position dynamics.

The results, presented in Fig. 2, reveal a striking contrast to the non-interacting regime, where no QME was observed. The introduction of onsite interactions induces clear QME signatures. The trace distance in panel 2(a) exhibits multiple crossover events, where systems initially farther from equilibrium overtake those starting closer, approaching the reference steady state more rapidly. This anomalous relaxation starkly contrasts with the monotonic ordering seen in the non-interacting case, confirming the emergence of QME.

The relative entropy in panel 2(b) supports this crossover phenomenon, showing that systems with higher initial hopping strengths, despite greater initial information-theoretic distance, achieve faster convergence at later times. This ordering reversal, absent in Sec. IV A, suggests that interactions enable systems with sufficient initial kinetic energy to overcome localization barriers, analogous to the classical Mpemba effect where

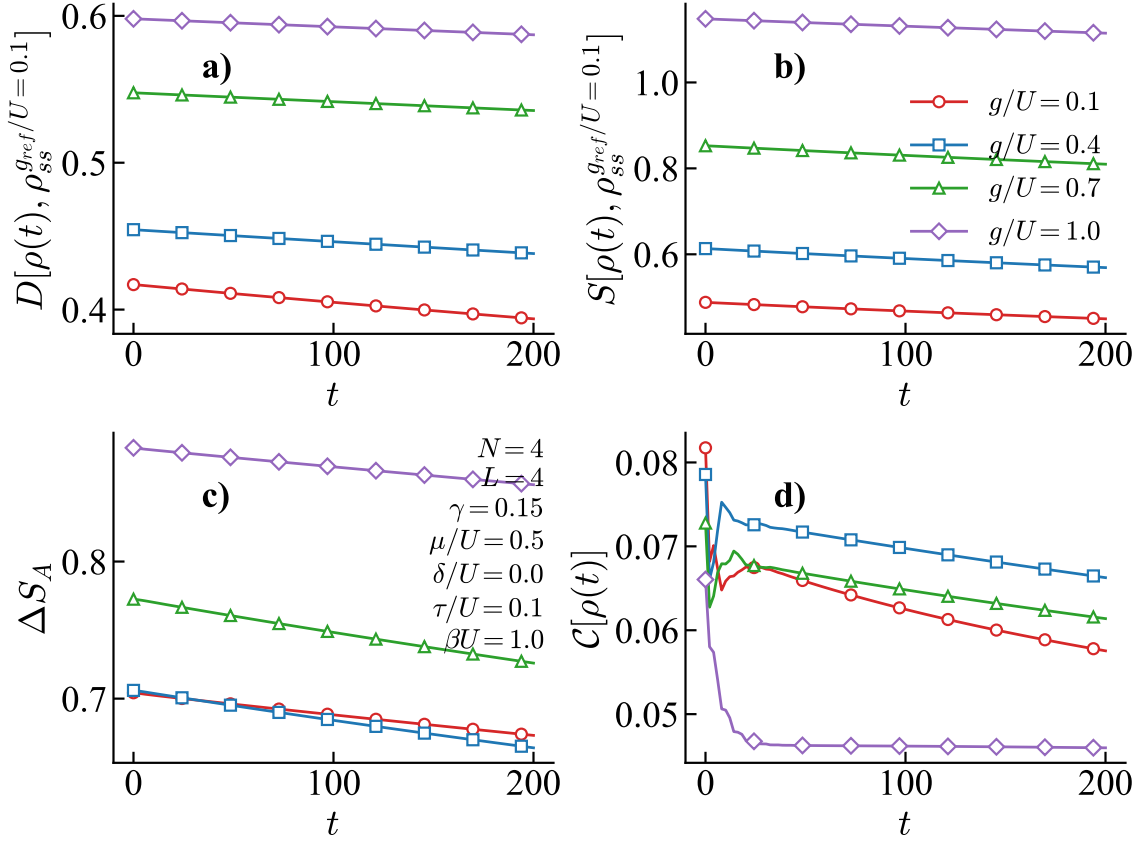


FIG. 3. Suppression of relaxation dynamics under Stark potential. Time evolution of quantum metrics for a Bose-Hubbard system with varying Stark field strengths g . A four-site system with fixed onsite interaction evolves from thermal initial states under Lindblad dynamics with local dephasing noise (rate γ/U). The reference steady state $\hat{\rho}_{ss}$ corresponds to a fixed Stark strength g_{ref} . All four metrics show systematic retardation of thermalization: (a) trace distance $D[\hat{\rho}_{ss}, \hat{\rho}(t)]$ exhibits maintained hierarchy with increased separation, (b) relative entropy $S[\hat{\rho}(t)||\hat{\rho}_{ss}]$ shows delayed convergence for stronger potentials, (c) entanglement asymmetry ΔS_A for bipartition A demonstrates persistent symmetry breaking, and (d) ℓ_1 -norm quantum coherence $\mathcal{C}[\hat{\rho}(t)]$ reveals coherence suppression under spatial inhomogeneity. Increasing Stark potential strength creates localization barriers that impede thermalization and prevent QME emergence. Parameters $\mu/U = 0.50$, $\tau/U = 0.1$, $\delta/U = 0$, fixed inverse temperature $\beta U = 1$ have been taken into consideration.

initially "hotter" systems relax faster.

Entanglement asymmetry dynamics in panel 2(c) provide key insight into the mechanism. Unlike the persistent symmetry breaking observed in the non-interacting regime, interactions facilitate efficient particle number symmetry restoration, with initially high-asymmetry states achieving lower final asymmetry. This indicates that QME arises from the interplay between interaction-induced correlations and dephasing-driven convergence to a particle-number-symmetric steady state.

The quantum coherence evolution in panel 2(d) further demonstrates that onsite interactions restructure decoherence pathways, enabling access to quantum superposition states that bridge efficiently to the steady state, unlike the conventional decoherence observed previously. This facilitates the counterintuitive relaxation behavior characteristic of QME.

These findings underscore the critical role of interactions in enabling QME. While the non-interacting system

in Sec. IV A exhibits conventional thermalization driven by initial proximity to equilibrium, onsite interactions introduce nonlinear coupling among quantum coherence, entanglement, and thermalization, driving anomalous relaxation dynamics. The results establish that quantum many-body correlations are essential for QME emergence in dissipative bosonic systems.

C. Clean Bose-Hubbard Regime with External Potentials

Having established the critical role of onsite interactions in facilitating the QME(QME) in Sec. IV B, we now investigate whether spatial inhomogeneity, introduced via external potentials, can serve as an alternative mechanism for anomalous relaxation dynamics, following the procedure outlined in Sec. III. Unlike interactions, which directly modify many-body correlations, external

potentials such as a linear Stark potential or random onsite disorder primarily affect the single-particle energy landscape while preserving the quantum many-body structure. This distinction, contrasted with the non-interacting and interacting clean regimes in Secs. [IV A](#) and [IV B](#), prompts the question: can spatial symmetry breaking induce the nonlinear relaxation pathways necessary for QME?

1. Stark Potential

We first consider a linear Stark potential, which introduces controllable site-to-site energy differences, creating a competition between gradient-induced localization and kinetic and thermal delocalization. We implement the procedure using a four-site bosonic chain with an equal number of particles, maintaining the onsite interaction and low hopping strength established in Sec. [IV B](#) to operate in the Mott insulating regime. Initial thermal states are prepared at a fixed inverse temperature, each characterized by a distinct Stark potential strength, and evolved under Lindblad dynamics with local dephasing noise acting on particle number operators. All systems converge toward a common reference steady state defined by a specific Stark potential strength. Relaxation dynamics are monitored using four quantum metrics: trace distance $D[\hat{\rho}_{ss}, \hat{\rho}(t)]$ for geometric distinguishability, relative entropy $S[\hat{\rho}(t) || \hat{\rho}_{ss}]$ for information-theoretic divergence, entanglement asymmetry ΔS_A for a chosen bipartition to assess particle number symmetry restoration, and ℓ_1 -norm quantum coherence $\mathcal{C}[\hat{\rho}(t)]$ in the Fock basis to capture quantum superposition dynamics.

The results, shown in Fig. [3](#), contrast sharply with the QME observed in the clean interacting regime. The trace distance in panel [3\(a\)](#) exhibits a hierarchical ordering, with stronger Stark potentials maintaining greater distance from the steady state throughout the evolution, indicating systematic thermalization impediments absent in Sec. [IV B](#). The relative entropy in panel [3\(b\)](#) corroborates this monotonic convergence hierarchy, showing slower information-theoretic equilibration for stronger potentials, unlike the crossover behavior previously observed. Entanglement asymmetry in panel [3\(c\)](#) reveals persistent symmetry breaking under stronger potentials, contrasting with the efficient symmetry restoration enabled by interactions alone. The quantum coherence dynamics in panel [3\(d\)](#) further indicate suppression of quantum superpositions, suggesting rapid decoherence or quantum coherence retention due to the inhomogeneous potential landscape, distinct from the interaction-driven quantum coherence pathways in Sec. [IV B](#). These findings suggest that Stark-induced spatial inhomogeneity inhibits QME by introducing localization barriers, unlike the anomalous relaxation facilitated by interactions.

2. Disordered Regime

To further explore the impact of spatial inhomogeneity, we investigate random onsite disorder in the absence of a Stark potential, maintaining the onsite interaction and low hopping strength from the previous cases. Initial thermal states are prepared at a fixed inverse temperature, each with a distinct disorder amplitude, and evolved under Lindblad dynamics toward a common reference steady state defined by a specific disorder strength. The same four quantum metrics are used to track relaxation dynamics.

The results, presented in Fig. [4](#), show that random disorder induces milder effects compared to the Stark potential. The trace distance in panel [4\(a\)](#) exhibits a modest convergence delay with increasing disorder amplitude, maintaining a hierarchical ordering similar to the Stark potential case but less pronounced than in Sec. [IV A](#)'s non-interacting regime. The relative entropy in panel [4\(b\)](#) supports this, indicating reduced relaxation efficiency due to localization effects, yet without the dramatic slowdowns seen with strong Stark potentials. Entanglement asymmetry in panel [4\(c\)](#) reveals disorder-induced translational symmetry breaking, with higher disorder sustaining greater asymmetry, though less severely than with Stark potentials. The quantum coherence dynamics in panel [4\(d\)](#) show slower decay at intermediate to late times, consistent with inhibited thermal mixing, but the overall behavior remains qualitatively similar across disorder strengths, lacking the QME crossovers observed in Sec. [IV B](#).

These findings highlight that both Stark potentials and random disorder suppress QME signatures by impeding thermalization, in contrast to the interaction-driven crossovers in the clean Bose-Hubbard regime. While interactions facilitate nonlinear relaxation pathways, spatial inhomogeneity introduces localization barriers that hinder anomalous dynamics, underscoring the necessity of many-body correlations for QME emergence in dissipative bosonic systems.

D. Disordered Bose-Hubbard Regime without Stark Potential

Following the exploration of Stark potentials in Sec. [IV C](#) and building on the interaction-driven QME observed in Sec. [IV B](#) and the non-interacting baseline in Sec. [IV A](#), we investigate whether random onsite disorder can induce the QME in the BHM, adhering to the procedure outlined in Sec. [IV](#). By maintaining zero Stark potential ($g = 0$), fixed onsite interaction, and low hopping strength in the Mott insulating regime, we isolate the effects of random disorder-induced translational symmetry breaking. This setup tests the universality of QME across different physical mechanisms, exploring whether disorder can overcome thermalization bottlenecks, akin to the interaction-driven pathways in Sec. [IV B](#), or if it

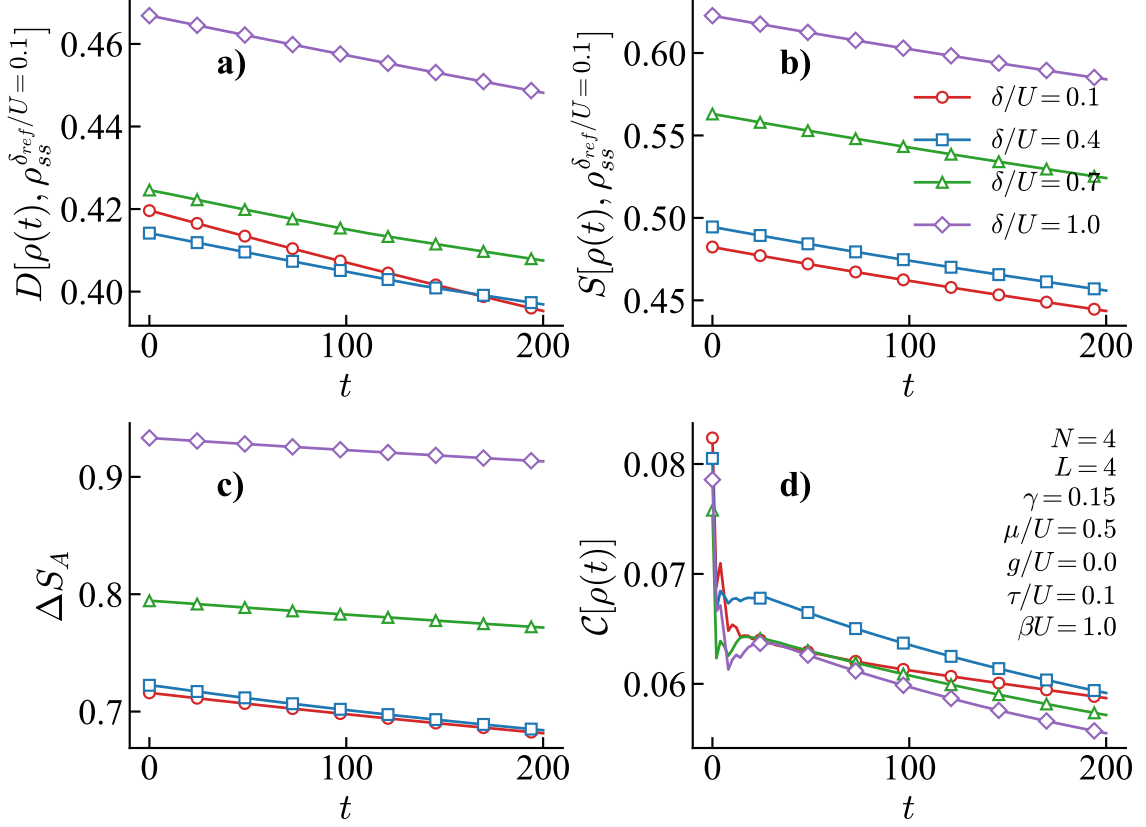


FIG. 4. Moderate thermalization suppression under random disorder. Relaxation dynamics of a Bose-Hubbard system with varying disorder amplitudes δ . A four-site system ($L = 4$, $N = 4$) with fixed onsite interaction evolves from thermal initial states under Lindblad dynamics with local dephasing noise (rate γ). The reference steady state $\hat{\rho}_{ss}$ corresponds to a fixed disorder amplitude δ_{ref} . All metrics indicate mild localization effects: (a) trace distance $D[\hat{\rho}_{ss}, \hat{\rho}(t)]$ shows modest convergence delays, (b) relative entropy $S[\hat{\rho}(t)||\hat{\rho}_{ss}]$ exhibits maintained relaxation hierarchy, (c) entanglement asymmetry ΔS_A for bipartition A reflects disorder-induced symmetry breaking, and (d) ℓ_1 -norm quantum coherence $C[\hat{\rho}(t)]$ demonstrates slower coherence decay. While random disorder impedes thermalization compared to the clean interacting case, its effects are less severe than Stark potential-induced localization, and no QME signatures are observed. Parameters $\mu = 0.50$, $U > 0$ (fixed), τ (fixed, low), $g = 0$, fixed inverse temperature $\beta U = 1$ have been assumed.

mirrors the localization effects seen with Stark potentials.

We implement the procedure using a four-site bosonic chain with an equal number of particles. Initial thermal states are prepared at a fixed inverse temperature, each characterized by a distinct random onsite disorder amplitude, and evolved under Lindblad dynamics with local dephasing noise acting on particle number operators, consistent with previous subsections. All systems converge toward a common reference steady state defined by a specific disorder amplitude. Relaxation dynamics are monitored using four quantum metrics: trace distance $D[\hat{\rho}_{ss}, \hat{\rho}(t)]$ for geometric distinguishability, relative entropy $S[\hat{\rho}(t)||\hat{\rho}_{ss}]$ for information-theoretic divergence, entanglement asymmetry ΔS_A for a chosen bipartition to assess particle number symmetry restoration, and ℓ_1 -norm quantum coherence $C[\hat{\rho}(t)]$ in the Fock basis to capture quantum superposition dynamics.

The results, presented in Fig. 4, reveal that random disorder suppresses QME signatures, akin to the Stark

potential case in Sec. IV C, but with milder effects compared to the pronounced localization observed there. The trace distance in panel 4(a) shows a modest but consistent convergence delay with increasing disorder amplitude, maintaining a hierarchical ordering, unlike the crossover events seen in the clean interacting regime (Sec. IV B). The relative entropy in panel 4(b) corroborates this, indicating reduced relaxation efficiency due to mild localization effects, less severe than the Stark potential's impact but similar to the conventional thermalization in Sec. IV A. Entanglement asymmetry in panel 4(c) reveals disorder-induced translational symmetry breaking, with higher disorder amplitudes sustaining greater asymmetry, though less persistently than with Stark potentials. The quantum coherence dynamics in panel 4(d) exhibit slower decay at intermediate to late times with increasing disorder, consistent with inhibited thermal mixing, yet lacking the dramatic suppression seen with strong Stark potentials.

These findings indicate that random onsite disorder disrupts thermalization by introducing mild localization effects, but it does not induce the nonlinear relaxation pathways necessary for QME, unlike the interaction-driven crossovers in Sec. IV B. Compared to the Stark potential's stringent localization barriers, disorder imposes less severe constraints, yet both external potentials contrast sharply with the anomalous dynamics enabled by many-body correlations. This underscores the necessity of interaction-driven mechanisms for QME emergence in dissipative bosonic systems.

V. CONCLUSION

This study systematically investigates the QME in a four-site BHM under various physical regimes, following an exact numerical procedure. Through exact numerical simulations of a four-site lattice with unit filling, employing Lindblad dynamics with local dephasing noise, we uncover the critical mechanisms governing anomalous relaxation dynamics and their dependence on many-body interactions and external potentials.

Our findings reveal that QME emerges prominently in the clean interacting regime, where onsite interactions induce nonlinear relaxation pathways, enabling initial states farther from equilibrium to overtake closer ones, as evidenced by crossover events in trace distance, relative entropy, entanglement asymmetry, and quantum coherence. This contrasts sharply with the non-interacting regime, where purely kinetic effects lead to conventional thermalization with monotonic convergence determined by initial proximity to the steady state. Considering linear Stark potential and random onsite disorder suppresses QME signatures by imposing localization barriers. Stark potential induces pronounced delay in relaxation, that is the indication of the symmetry breaking and suppressing quantum coherence, while random disorder causes milder convergence delays, yet both fail to produce the anomalous dynamics observed in the interaction-driven case.

These results underscore that many-body correlations are essential for QME in dissipative bosonic systems, as they facilitate efficient symmetry restoration and quantum coherence dynamics, absent in non-interacting or perturbed systems. The consistent behavior across multiple quantum metrics validates the robustness of our findings, with entanglement asymmetry emerging as a particularly sensitive probe of symmetry restoration dynamics. Our work highlights the delicate interplay between interactions, spatial inhomogeneity, and dissipation in controlling quantum thermalization, offering insights for experimental platforms such as ultracold atoms in optical lattices.

Our results open avenues for future studies in larger system sizes to assess scalability, dissipation mechanisms, and many-body localization, potentially uncovering new strategies for controlling non-equilibrium quantum dynamics. By advancing the theoretical understanding of QME, these findings lay the groundwork for engineering anomalous relaxation in quantum simulation platforms.

ACKNOWLEDGMENTS:

This work was supported by the Qatar National Research Fund (QNRF) under grant number ARG01-0603-230468. H.A.Z. acknowledges the financial support provided under the postdoctoral fellowship program of P. J. Šafárik University in Košice, Slovakia.

DATA AVAILABILITY:

All data generated or analyzed during this study are included in this published article.

COMPETING INTERESTS:

The authors declare no competing interests.

-
- [1] E. B. Mpemba and D. G. Osborne, *Cool?*, *Physics Education* **4**, 172 (1969).
 - [2] Aristotle and S. H. D. P. LEE, *Aristotle Meteorologica. With an English Translation by Henry DP Lee* (London; Harvard University Press: Cambridge, Mass., 1952).
 - [3] R. Descartes, *A discourse on method* (JM Dent & Sons Limited, 1912).
 - [4] F. Bacon, *Novum organum*, edited by m, Joseph Devey (New York: PF Collier, 1902) (1902).
 - [5] H. C. Burridge and P. F. Linden, Questioning the mpemba effect: hot water does not cool more quickly than cold, *Scientific Reports* **6**, 37665 (2016).
 - [6] J. Bechhoefer, A. Kumar, and R. Chérite, A fresh understanding of the mpemba effect, *Nature Reviews Physics* **3**, 534 (2021).
 - [7] Y.-H. Ahn, H. Kang, D.-Y. Koh, and H. Lee, Experimental verifications of mpemba-like behaviors of clathrate hydrates, *Korean Journal of Chemical Engineering* **33**, 1903 (2016).
 - [8] C. Hu, J. Li, S. Huang, H. Li, C. Luo, J. Chen, S. Jiang, and L. An, Conformation directed mpemba effect on polylactide crystallization, *Crystal Growth & Design* **18**, 5757 (2018).
 - [9] P. Chaddah, S. Dash, K. Kumar, and A. Banerjee, Over-taking while approaching equilibrium, *arXiv preprint arXiv:1011.3598* (2010).
 - [10] P. A. Greaney, G. Lani, G. Cicero, and J. C. Grossman, Mpemba-like behavior in carbon nanotube resonators,

- Metallurgical and Materials Transactions A **42**, 3907 (2011).
- [11] A. Lasanta, F. Vega Reyes, A. Prados, and A. Santos, When the hotter cools more quickly: Mpemba effect in granular fluids, *Physical review letters* **119**, 148001 (2017).
 - [12] T. Keller, V. Torggler, S. B. Jäger, S. Schütz, H. Ritsch, and G. Morigi, Quenches across the self-organization transition in multimode cavities, *New Journal of Physics* **20**, 025004 (2018).
 - [13] Z. Lu and O. Raz, Nonequilibrium thermodynamics of the markovian mpemba effect and its inverse, *Proceedings of the National Academy of Sciences* **114**, 5083 (2017).
 - [14] I. Klich, O. Raz, O. Hirschberg, and M. Vucelja, Mpemba index and anomalous relaxation, *Physical Review X* **9**, 021060 (2019).
 - [15] J. Zhang, G. Xia, C.-W. Wu, T. Chen, Q. Zhang, Y. Xie, W.-B. Su, W. Wu, C.-W. Qiu, P.-X. Chen, *et al.*, Observation of quantum strong mpemba effect, *Nature Communications* **16**, 301 (2025).
 - [16] F. Carollo, A. Lasanta, and I. Lesanovsky, Exponentially accelerated approach to stationarity in markovian open quantum systems through the mpemba effect, *Physical Review Letters* **127**, 060401 (2021).
 - [17] S. Longhi, Quantum mpemba effect from non-normal dynamics, *Entropy* **27**, 581 (2025).
 - [18] F. Ares, P. Calabrese, and S. Murciano, The quantum mpemba effects, *arXiv preprint arXiv:2502.08087* (2025).
 - [19] Y. Yu, T. Jin, L. Zhang, K. Xu, and H. Fan, Tuning the quantum mpemba effect in isolated system by initial state engineering, *arXiv preprint arXiv:2505.02040* (2025).
 - [20] S. Longhi, Mpemba effect and super-accelerated thermalization in the damped quantum harmonic oscillator, *Quantum* **9**, 1677 (2025).
 - [21] L. K. Joshi, J. Franke, A. Rath, F. Ares, S. Murciano, F. Kranzl, R. Blatt, P. Zoller, B. Vermersch, P. Calabrese, *et al.*, Observing the quantum mpemba effect in quantum simulations, *Physical Review Letters* **133**, 010402 (2024).
 - [22] S. Aharony Shapira, Y. Shapira, J. Markov, G. Teza, N. Akerman, O. Raz, and R. Ozeri, Inverse mpemba effect demonstrated on a single trapped ion qubit, *Physical Review Letters* **133**, 010403 (2024).
 - [23] A. Ali, M. Hussain, S. Al-Kuwari, M. Rahim, H. Kuniyil, S. M. Hosseiny, J. Seyed-Yazdi, H. A. Zad, and S. Haddadi, Coherence, transport, and chaos in 1d bose-hubbard model: Disorder vs. stark potential, *arXiv preprint arXiv:2505.19071* (2025).
 - [24] M. A. Nielsen and I. L. Chuang, *Quantum computation and quantum information* (Cambridge university press, 2010).
 - [25] M. Moroder, O. Culhane, K. Zawadzki, and J. Goold, Thermodynamics of the quantum mpemba effect, *Physical Review Letters* **133**, 140404 (2024).
 - [26] C. Rylands, E. Vernier, and P. Calabrese, Dynamical symmetry restoration in the heisenberg spin chain, *Journal of Statistical Mechanics: Theory and Experiment* **2024**, 123102 (2024).
 - [27] S. Liu, H.-K. Zhang, S. Yin, and S.-X. Zhang, Symmetry restoration and quantum mpemba effect in symmetric random circuits, *Physical Review Letters* **133**, 140405 (2024).
 - [28] H.-Y. Huang, R. Kueng, and J. Preskill, Predicting many properties of a quantum system from very few measurements, *Nature Physics* **16**, 1050 (2020).
 - [29] T. Brydges, A. Elben, P. Jurcevic, B. Vermersch, C. Maier, B. P. Lanyon, P. Zoller, R. Blatt, and C. F. Roos, Probing rényi entanglement entropy via randomized measurements, *Science* **364**, 260 (2019).
 - [30] T. Baumgratz, M. Cramer, and M. B. Plenio, Quantifying coherence, *Phys. Rev. Lett.* **113**, 140401 (2014).
 - [31] N. Lambert, E. Giguère, P. Menczel, B. Li, P. Hopf, G. Suárez, M. Gali, J. Lishman, R. Gadhvi, R. Agarwal, A. Galicia, N. Shammah, P. Nation, J. R. Johansson, S. Ahmed, S. Cross, A. Pitchford, and F. Nori, Qutip 5: The quantum toolbox in python, (2024), [arXiv:2412.04705 \[quant-ph\]](https://arxiv.org/abs/2412.04705).
 - [32] J. Johansson, P. Nation, and F. Nori, Qutip 2: A python framework for the dynamics of open quantum systems, *Computer Physics Communications* **184**, 1234 (2013).
 - [33] J. Johansson, P. Nation, and F. Nori, Qutip: An open-source python framework for the dynamics of open quantum systems, *Computer Physics Communications* **183**, 1760 (2012).